The Astrophysical Journal, 872:85 (13pp), 2019 February 10 https://doi.org/10.3847/1538-4357/aafbed

Testing Systematics of *Gaia* DR2 Parallaxes with Empirical Surface Brightness: Color Relations Applied to Eclipsing Binaries

Dariusz Graczyk[1,2,3], Grzegorz Pietrzyński[2,3], Wolfgang Gieren[1,2], Jesper Storm[4], Nicolas Nardetto[5], Alexandre Gallenne[5,6], Pierre F. L. Maxted[7], Pierre Kervella[8,9], Zbigniew Kołaczkowski[3,10], Piotr Konorski[11], Bogumił Pilecki[3], Bartłomiej Zgirski[3], Marek Górski[2], Ksenia Suchomska[3], Paulina Karczmarek[1,2], Mónica Taormina[3], Piotr Wielgórski[3], Weronika Narloch[1,2,3], Radosław Smolec[3], Rolf Chini[12,13], and Louise Breuval[9]

[1] Millennium Institute of Astrophysics (MAS), Chile
[2] Universidad de Concepción, Departamento de Astronomia, Casilla 160-C, Concepción, Chile; darek@astro-udec.cl
[3] Centrum Astronomiczne im. Mikołaja Kopernika (CAMK), PAN, Bartycka 18, 00-716 Warsaw, Poland; darek@ncac.torun.pl
[4] Leibniz-Institut für Astrophysik Potsdam, An der Sternwarte 16, D-14482 Potsdam, Germany
[5] Université Côte d'Azur, Observatoire de la Côte d'Azur, CNRS, Laboratoire Lagrange, UMR7293, Nice, France
[6] European Southern Observatory, Alonso de Córdova 3107, Casilla 19001, Santiago 19, Chile
[7] Astrophysics Group, Keele University, Staffordshire, ST5 5BG, UK
[8] Unidad Mixta Internacional Franco-Chilena de Astronomía (CNRS Umi 3386), Departamento de Astronomía, Universidad de Chile, Camino El Observatorio 1515, Las Condes, Santiago, Chile
[9] LESIA (UMR 8109), Observatoire de Paris, PSL Research University, CNRS, UPMC, Univ. Paris-Diderot, 5 place Jules Janssen, F-92195 Meudon, France
[10] Instytut Astronomiczny, Uniwersytet Wrocławski, Kopernika 11, 51-622 Wrocław, Poland
[11] Obserwatorium Astronomiczne, Uniwersytet Warszawski, Al. Ujazdowskie 4, 00-478, Warsaw, Poland
[12] Ruhr University Bochum, Faculty of Physics and Astronomy, Astronomical Institute, D-44801 Bochum, Germany
[13] Instituto de Astronomia, Universidad Catolica del Norte Avenida Angamos 0610, Antofagasta, Chile
Received 2018 October 30; revised 2018 December 1; accepted 2018 December 12; published 2019 February 13

Abstract

Using a sample of 81 galactic, detached eclipsing binary stars we investigated the global zero-point shift of their parallaxes with the *Gaia* Data Release 2 (DR2) parallaxes. The stars in the sample lay in a distance range of 0.04–2 kpc from the Sun. The photometric parallaxes $\varpi_{\rm Phot}$ of the eclipsing binaries were determined by applying a number of empirical surface brightness–color (SBC) relations calibrated on optical-infrared colors. For each SBC relation we calculated the individual differences $d\varpi_i = (\varpi_{Gaia} - \varpi_{\rm Phot})_i$ and then we calculated unweighted and weighted means. As the sample covers the whole sky we interpret the weighted means as the global shifts of the *Gaia* DR2 parallaxes with respect to our eclipsing binary sample. Depending on the choice of the SBC relation the shifts vary from −0.094 to −0.025 mas. The weighted mean of the zero-point shift from all colors and calibrations used is $d\varpi = -0.054 \pm 0.024$ mas. However, the SBC relations based on $(B-K)$ and $(V-K)$ colors, which are the least reddening dependent and have the lowest intrinsic dispersions, give a zero-point shift of $d\varpi = -0.031 \pm 0.011$ mas in full agreement with results obtained by Lindegren et al. and Arenou et al. Our result confirms the global shift of *Gaia* DR2 parallaxes of $d\varpi = -0.029$ mas reported by the *Gaia* team, but we do not confirm the larger zero-point shift reported by a number of follow-up papers.

Key words: binaries: eclipsing – parallaxes – stars: distances

Supporting material: machine-readable tables

1. Introduction

The *Gaia* mission (Gaia Collaboration et al. 2016) is a milestone in understanding the Milky Way structure and its chemo-dynamical evolution, but it is also extremely important for the recalibration of standard candles and standard rulers used to construct the extragalactic distance ladder. A number of studies devoted to the recalibration of Cepheids and RR Lyr stars with *Gaia* Data Release 2 (DR2) parallaxes has already appeared (e.g., Groenewegen 2018; Muraveva et al. 2018).

The possible global systematics of the *Gaia* DR2 parallaxes were evaluated with different methods by the *Gaia* consortium. Lindegren et al. (2018) used quasars and internal validation solutions to estimate the systematics and reported that the parallaxes are, on average, about 0.03 mas too small, and that some local significant correlations of parallaxes occur. Arenou et al. (2018) made a comparison of *Gaia* DR2 parallaxes with a number of external catalogs to evaluate the global shift. Individual shifts vary from -0.118 ± 0.003 mas (*HIPPARCOS*) to $+0.09 \pm 0.07$ mas (Phoenix dwarf), where the minus sign signifies that *Gaia* parallaxes are too small. However, most catalogs point to a global systematic offset of about −0.03 mas, e.g., comparisons with the Large and Small Magellanic Cloud star catalogs, which have the smallest formal uncertainties, yield shifts of -0.0380 ± 0.0004 mas and -0.0268 ± 0.0006 mas, respectively.

The global shift was also evaluated by a number of external works. A comparison with distance moduli of 50 Galactic cepheids derived from *HST* photometry resulted in an estimate of global zero-point offset of *Gaia* DR2 parallaxes of -0.046 ± 0.013 mas (Riess et al. 2018). Using a sample of 3475 red giant branch stars in the *Kepler* field from the APOKASC-2 catalog and asteroseismic relations, Zinn et al. (2018) found a systematic shift of -0.053 ± 2(stat) ± 1(syst) mas. The derived shift is specific to the *Kepler* field but it would also be a measure of the global zero-point shift. Another approach was presented by Stassun & Torres (2018) who used the eclipsing binary method. They calculated observed reddening-free bolometric fluxes $F_{\rm bol}$ by fitting the spectral energy distribution and compared them to the bolometric luminosities $L_{\rm bol}$ to obtain distances. Using a subsample of 89 suitable

Table 1
Basic Data on the Selected Detached Eclipsing Binaries

Name	*GAIA* DR2 ID	R.A.$_{(2000)}$ h:m:s	Decl.$_{(2000)}$ deg:m:s	V (mag)	Spectral Type	Orbital Period (days)	*GAIA* DR2 Parallax (mas)
MU Cas	429158427922077184	00:15:51.560	+60:25:53.64	10.808 ± 0.007	B5V+B5V	9.652949	0.453 ± 0.040
YZ Cas	539047365205648128	00:45:39.077	+74:59:17.06	5.653 ± 0.015	A2m+F2V	4.4672235	10.473 ± 0.094
V459 Cas	522461335380031104	01:11:29.913	+61:08:48.07	10.322 ± 0.003	A1V+A1V	8.4582538	1.304 ± 0.048
V505 Per	455772347387763840	02:21:12.964	+54:30:36.28	6.889 ± 0.016	F5V+F5V	4.222020	15.970 ± 0.039
DN Cas	513431183821175936	02:23:11.540	+60:49:50.18	9.878 ± 0.010	O8V+B0V	2.31095111	0.485 ± 0.032

(This table is available in its entirety in machine-readable form.)

eclipsing binaries from their catalog (Stassun & Torres 2016) they derived a global shift of -0.082 ± 0.033 mas. The method used by Stassun & Torres (2018) is, from a theoretical point of view, the most robust one because it utilizes a very wide range of photometry from UV to midinfrared. However, the $L_{\rm bol}$ are calculated from the effective temperature of each component and this radiative parameter is almost always the least constrained fundamental parameter of an eclipsing binary. There are two main reasons for this: (1) the wide range of methods used to determine effective temperatures that exhibit significantly different zero-points of the resulting temperature scales, and (2) the notorious difficulty in establishing an absolute temperature scale with a precision better than 1% (e.g., Casagrande et al. 2014). Thus from a practical point of view the method used by Stassun & Torres (2018) is not the optimal one because it has some systematics that are still difficult to properly evaluate. The need of an eclipsing binary approach, which would minimize systematic effects and would be based on direct and precise empirical relations, was the prime motivation for this work. As in our previous work (Graczyk et al. 2017, hereafter G17) we focus on an application of surface brightness–color relations.

2. The Sample

We extended the sample of 35 eclipsing binaries compiled by G17 by searching for detached systems in the literature suitable for a precise distance determination. In order to make the extension we used catalogs of eclipsing binary systems compiled by a number of authors: Bilir et al. (2008), Torres et al. (2010), Eker et al. (2014), Southworth (2015), and Stassun & Torres (2016).

We used the same selection criteria as in G17; however, we relaxed the condition on a volume-limited sample ($d < 300$ pc) by also accepting more distant systems. Because the β Aur system is too bright to have a *Gaia* parallax, and AI Phe is a confirmed triple system (M. Konacki 2019, private communication) we drop these systems from our sample. We also included a system from our unpublished work: AL Dor. Following G17 we retained systems with a fractional precision of recent *Gaia* DR2 parallaxes (Gaia Collaboration et al. 2016, 2018; Lindegren et al. 2018) better then 10%. A trigonometric parallax ϖ with a fractional error $f = \sigma_{\varpi}/\varpi$ smaller than 0.1 is a good and weakly biased estimator of the true distance (e.g., Bailer-Jones 2015; Bailer-Jones et al. 2018). In our sample only two early and distant systems have f marginally larger than 0.1, i.e., EM Car and DW Car. Most of the sample systems have fractional errors of their parallaxes smaller than 0.06 for which any bias can be completely neglected. Finally our sample contains 81 systems (51 on the northern hemisphere and 30 on the southern one). Their basic parameters are presented in Table 1 and the distribution of the parallax fractional errors is presented in Figure 1.

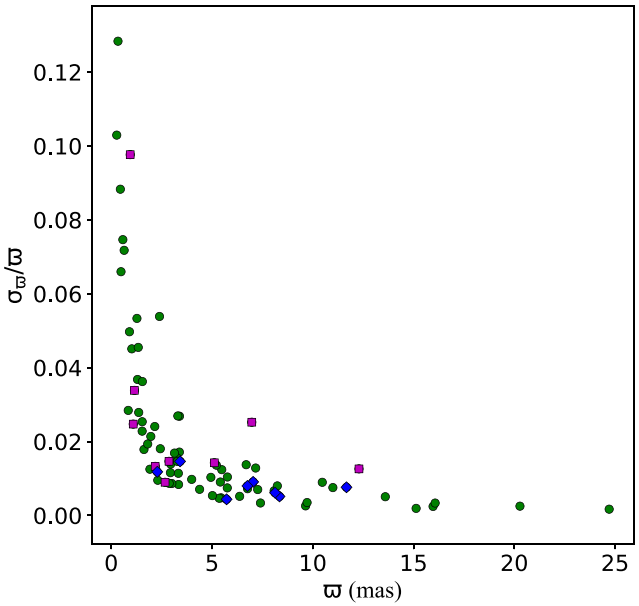

Figure 1. Distribution of fractional error of *Gaia* DR2 parallaxes for all 81 eclipsing binaries in our sample. Nine systems with suspected binary motion detection or calibration problems are denoted by squares. Eight stars with the significant PMa are denoted by diamonds.

Arenou et al. (2018) proposed three quality controls to estimate reliability of astrometric solutions of *Gaia* DR2; they are defined by their Equations (1)–(3). Those quality controls help to filter out most spurious astrometric solutions, but they filter out also some well-defined solutions. In our sample, 9 stars do not fulfill the first criterium (possible double stars, suspected binary motion, or calibration problems) and 7 other stars do not fulfill the third criterium (i.e., `visibility_periods_used` < 8). However, the third criterium is useful mostly to very crowded fields in the Bulge and as no star in our sample is there, we kept these 7 systems during analysis. The 9 stars that do not fulfill the first criterium are denoted as squares in Figure 1. Only 3 of them have the relative parallax uncertainty larger by a factor of two than expected. We investigated our sample further by looking for the proper motion anomaly (PMa; Kervella et al. 2019), which could be a sign of a photocenter movement or a third body in a system. The PMa results from a comparison of the proper motion

Table 2
Parameters of the Wilson–Devinney Models

Eclipsing Binary	Input Parameters: RV Semiamplitude K_1 (km s^{-1})	RV Semiamplitude K_2 (km s^{-1})	Orientation of the Orbit e	Orientation of the Orbit ω (rad)	Orientation of the Orbit i (deg)	Fractional Radius r_1	Fractional Radius r_2	Effective Temperature T_1 (K)	Effective Temperature T_2 (K)	References	WD Model Parameters: Semimajor Axis ($R_\odot$)	Mass Ratio	Ω_1	Ω_2
MU Cas	107.7(1.0)	105.8(9)	0.1930(3)	0.234(7)	87.02(7)	0.0917(9)	0.1048(10)	15900(500)	15525(500)	(1)	40.0234	1.0180	12.173	10.952
YZ Cas	73.05(19)	124.78(27)	0.0	⋯	88.33(7)	0.14456(56)	0.07622(33)	9520(120)	6880(240)	(2)	17.4753	0.5854	7.5141	8.8912
V459 Cas	81.70(60)	83.90(60)	0.0243(4)	4.19(1)	89.47(1)	0.07260(30)	0.07100(30)	9140(300)	9085(300)	(3)	27.6786	0.9738	14.776	14.757
V505 Per	89.01(8)	90.28(9)	0.0	⋯	87.95(4)	0.0860(9)	0.0846(9)	6512(21)	6460(30)	(4)	14.9715	0.9859	12.618	12.665
DN Cas	211(3)	292(5)	0.0	⋯	77.20(20)	0.3070(20)	0.2460(20)	32100(1000)	28500(1100)	(5)	23.5613	0.7226	4.0372	4.1129

References. (1) Lacy et al. (2004b); (2) Pavlovski et al. (2014); (3) Lacy et al. (2004a); (4) Tomasella et al. (2008b); (5) Bakiş et al. (2016); (6) this paper; (7) Clausen et al. (2001); (8) Southworth et al. (2011); (9) Tomasella et al. (2008a); (10) Andersen et al. (1991); (11) Gallenne et al. (2016); (12) Lacy et al. (2006); (13) Munari et al. (2004); (14) Southworth et al. (2005); (15) Groenewegen et al. (2007); (16) David et al. (2016); (17) Lacy & Frueh (1985); (18) Maxted et al. (2015); (19) Lacy (2002); (20) Ribas et al. (1999); (21) Imbert (2002); (22) Clausen et al. (2010); (23) Andersen et al. (1989); (24) Hełminiak et al. (2009); (25) Andersen et al. (1987a); (26) Torres et al. (2014); (27) Sabby et al. (2011); (28) Khaliullin et al. (2001); (29) Tomkin & Fekel (2006); (30) Southworth et al. (2005); (31) Kirkby-Knet et al. (2018); (32) Torres et al. (2015); (33) Lacy et al. (2008); (34) Popper et al. (1985); (35) Lacy et al. (2000); (36) Lacy (1987); (37) Williamon et al. (2004); (38) Henry et al. (2006); (39) Clausen et al. (2008); (40) Sowell et al. (2012); (41) Sandquist et al. (2018); (42) Yakut et al. (2007); (43) Albrecht et al. (2014); (44) Bakiş et al. (2008); (45) Andersen & Vaz (1984); (46) Andersen et al. (1983); (47) Andersen et al. (1975); (48) Giuricin et al. (1980); (49) Southworth & Clausen (2007); (50) Andersen & Clausen (1989); (51) Stickland et al. (1994); (52) Ratajczak et al. (2010); (53) Clausen et al. (2007); (54) Albrecht et al. (2013); (55) Lacy & Fekel (2011); (56) Andersen (1975); (57) Gronbech et al. (1977); (58) Walker & Chambliss (1983); (59) Andersen et al. (1984); (60) Latham et al. (1996); (61) Lacy (1997); (62) Popper (1998); (63) Andersen et al. (1993); (64) Budding et al. (2015); (65) Lacy et al. (2012); (66) North et al. (1997); 67) Andersen et al. (1985); (68) Fekel et al. (2011); (69) Pribulla et al. (2018); (70) Torres et al. (2009); (71) Lacy & Fekel (2014); (72) Suchomska et al. (2015); (73) Popper (1971); (74) Clausen et al. (1986); (75) Imbert (1985); (76) Lacy et al. (2012); (77) Popper (1982); (78) Albrecht et al. (2009); (79) Popper et al. (1986); (80) Imbert (1986); (81) Lacy et al. (1989); (82) Veramendi & González (2015); (83) Sandquist et al. (2016); (84) Andersen et al. (1987b); (85) Albrecht et al. (2007); (86) Torres et al. (2017); (87) Pavlovski et al. (2009); (88) Tkachenko et al. (2014); (89) Hełminiak et al. (2015); (90) Rawls et al. (2016); (91) Torres et al. (2010); (92) Lacy & Frueh (1987); (93) Harmanec et al. (2014); (94) Torres et al. (2000); (95) Torres & Lacy (2009); (96) Imbert (1987); (97) Clausen (1991); (98) Lester & Gies (2018); (99) Popper (1987); (100) Griffin (2013); (101) Southworth (2013); (102) Graczyk et al. (2016); (103) Torres et al. (1999); (104) Vos et al. (2012); (105) Barembaum & Etzel (1995); (106) Lacy et al. (2004c); (107) Popper (1983); (108) Demircan et al. (1994); (109) Clausen et al. (2010); (110) Lacy et al. (2014); (111) Çakirli et al. (2009).

(This table is available in its entirety in machine-readable form.)

Table 3
Corrections to Original 2MASS Magnitudes

ID	K (mag)	H (mag)	J (mag)
GG Lup	−0.345	−0.342	−0.334
KX Cnc	−0.426	−0.427	−0.429
WZ Oph	−0.535	−0.536	−0.540
YZ Cas	−0.162	−0.155	−0.137
BW Aqr	−0.524	−0.526	−0.532
SZ Cen	−0.454	−0.458	−0.467
V442 Cyg	−0.283	−0.283	−0.283
ASAS1800	−0.512	−0.505	−0.493
DW Car	−0.464	−0.465	−0.467

vectors at the *Hipparcos* and *Gaia* epoch with the mean proper motion computed from a coordinate shift between *Hipparcos* and *Gaia* epochs. We found a significant (SNR = 5) detection of the PMa for 8 stars, but interestingly none of them are common with the subsample of 9 suspected stars. The stars with the PMa are denoted as diamonds in Figure 1. All of them have well-defined 5-parametric astrometric solutions, and the PMa, if confirmed with later *Gaia* data releases, is likely due to long-period changes caused by an unrecognized triple companion.

2.1. Photometry

2.1.1. Optical

We used Tycho-2 B_T and V_T photometry (Høg et al. 2000) downloaded from Vizier (Ochsenbein et al. 2000).[14] The Tycho photometry was subsequently transformed onto the Johnson system using the method outlined by Bessell (2000). Whenever possible we used Johnson B, V photometry from the compilation of Mermilliod (1997) and also absolute optical photometry from literature sources.

2.1.2. Near Infrared

We used NIR JHK_S photometry of the Two Micron All Sky Survey (2MASS; Skrutskie et al. 2006) from Vizier.[15] For the purpose of using the SBC relations based on the $(V-K)$ color expressed on the Johnson photometric system we transformed the 2MASS magnitudes using the equations given in Bessell & Brett (1988) and Carpenter (2001).[16] The transformation equations are as follows:

$$K_J - K_{2M} = 0.037 - 0.017(J-K)_{2M} - 0.007(V-K)_{2M} \quad (1)$$

$$(J-K)_J = 1.064(J-K)_{2M} + 0.006 \quad (2)$$

$$(H-K)_J = 1.096(H-K)_{2M} - 0.027. \quad (3)$$

3. Method

3.1. Collection of Fundamental Parameters

For each system we collected orbital and photometric parameters from the literature including the most recent publications. We were searching for basic parameters describing dynamical and geometrical parameters of each system: the radial velocity semiamplitudes $K_{1,2}$, the orbital period P, the orbital inclination i, the eccentricity e, the longitude of periastron ω, and the photometric relative radii $r_{1,2}$. These parameters were supported by radiative parameters: the effective temperatures $T_{1,2}$ of both components. The radiative parameters are usually known with the least precision and accuracy. Whenever several papers independently presented the analysis of a given eclipsing binary we adopted the weighted mean for the parameters. However, if there was a significant improvement on the precision of parameters reported in one of papers, then we used only values from that paper. It turned out that we could not always directly trace all the above parameters from literature sources. In some cases when modeling of an eclipsing binary was done with numerical codes based on the Roche formalism (the Wilson–Devinney (WD) code, the ELC code, etc.) we had to calculate relative radii and radial velocity semiamplitudes from the absolute dimensions presented in the relevant papers. The collected parameters are summarized in Table 2.

3.2. The WD Model of the Systems

For the purpose of obtaining homogenous parameters for the eclipsing binary sample we decided to create a model of each system following G17. The models were built using the WD code version 2007 (Wilson & Devinney 1971; Wilson 1979, 1990; van Hamme & Wilson 2007) while parameters of the models were based on solutions published in the literature (see Section 3.1). All models were checked for internal consistency of the parameters and it turned out that in many cases they had to be fine-tuned. In particular, the temperature ratio and the absolute temperature scale, being important for a precise prediction of infrared light ratios, were inspected carefully.

The procedure was as follows. Dynamical and geometrical parameters were transformed into the semimajor axis of the system a, the mass ratio q and into dimensionless Roche potentials $\Omega_{1,2}$ using equations given in Torres et al. (2010) and Wilson (1979). Both Ω and q are parameters directly fitted or used within the WD program. We usually fixed the temperature of the primary star T_1 and then, using published light ratios in different photometric bands, we adjusted the temperature of the companion T_2. In very few cases, however, we also rederived T_1 using two temperature–color calibrations (Flower 1996; Worthey & Lee 2011). However the temperature shifts are small and within errors given in the literature. None of the eclipsing binaries in our sample has infrared *J, H, K* light curves suitable for deriving direct light ratios in those bands. Thus, in order to calculate intrinsic infrared colors of the components of each system we employed eclipsing binary models based on optical light curves and we extrapolated them into the infrared. The extrapolation was done using the atmosphere approximation within the WD code, which uses precomputed intensities based on Kurucz's ATLAS9 models (Kurucz 1993).

The rotation parameter $F_{1,2}$ was kept to 1 (synchronous rotation), unless there was a direct spectroscopic determination of F significantly different from unity. The albedo A and the gravity brightening g were set in a standard way for a convective atmosphere cooler then 7200 K and radiative ones for a hotter surface temperature. This was done only for the sake of consistency because the two parameters have negligible effect on the light ratios. The input and derived parameters used to create the appropriate WD models are listed in Table 2.

[14] http://vizier.u-strasbg.fr: I/259/tyc2.
[15] http://vizier.u-strasbg.fr: II/281/2mass6x.
[16] http://www.astro.caltech.edu/~jmc/2mass/v3/transformations/

Table 4
Physical and Photometric Parameters of Individual Components Used to Derive Photometric Parallaxes

Eclipsing Binary	$E(B-V)$ (mag)	Radius ($R_\odot$)		Observed Magnitudes					Light Ratios				
		R_1	R_2	B (mag)	V (mag)	J (mag)	H (mag)	K (mag)	B	V	J	H	K
MU Cas	0.478(10)	3.670(43)	4.194(48)	11.112(9)	10.808(7)	10.170(23)	10.092(23)	10.050(16)	1.253	1.257	1.273	1.276	1.277
YZ Cas	0.015(10)	2.526(11)	1.332(6)	5.715(26)	5.660(15)	5.490(20)	5.502(42)	5.475(22)	0.061	0.088	0.168	0.200	0.205
V459 Cas	0.246(24)	2.009(13)	1.965(13)	10.591(9)	10.322(3)	9.791(23)	9.715(25)	9.668(16)	0.936	0.941	0.949	0.950	0.951
V505 Per	0.003(5)	1.288(14)	1.267(14)	7.269(30)	6.846(20)	6.120(70)	5.793(39)	5.795(21)	0.924	0.935	0.952	0.958	0.959
DN Cas	0.917(50)	7.233(96)	5.796(82)	10.495(18)	9.878(10)	8.413(25)	8.217(19)	8.132(24)	0.492	0.500	0.521	0.527	0.529

(This table is available in its entirety in machine-readable form.)

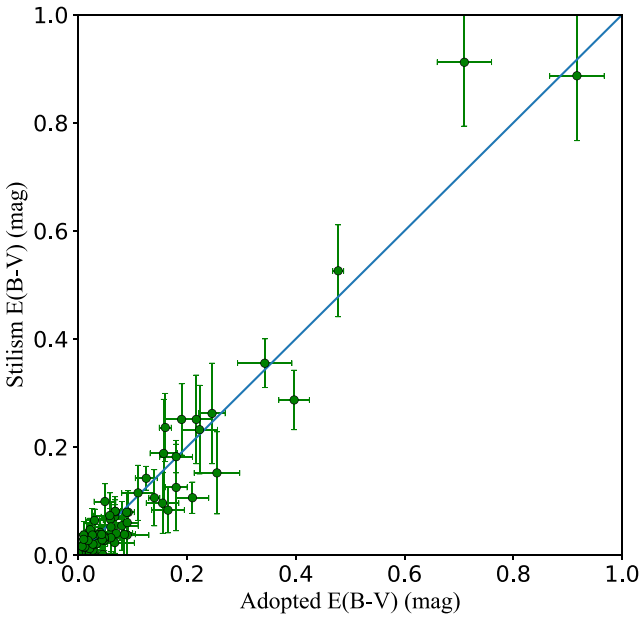

Figure 2. The comparison of our adopted reddening estimates with 3D *Stilism* extinctions.

3.3. Correction of 2MASS Magnitudes Taken during Eclipses

Nine systems from our sample have 2MASS observations taken during the eclipses. To account for the light lost during the minima we used our WD models to calculate the appropriate corrections, which are given in Table 3.

3.4. Reddening

Reddenings to each object were taken from the literature. We also derived independently values of $E(B-V)$ using the extinction maps of Schlegel et al. (1998) following the prescription given in Suchomska et al. (2015). Usually as a final value of the extinction we used an average, unless determinations were discrepant or we have at our disposal only one reddening estimate. The adopted reddenings are reported in Table 4. To check them we compared them with independent extinction estimates from 3D extinction maps from *Stilism* (Lallement et al. 2014; Capitanio et al. 2017)—see Figure 2. On average *Stilism* extinctions are slightly smaller, but an overall agreement is good, and although the spread is quite large both sets of reddenings are consistent within errors.

3.5. Intrinsic Magnitudes

In Table 4 we summarize all parameters used to derive the intrinsic photometric indexes of the component stars. In order to calculate them the photometry was dereddened using the mean Galactic interstellar extinction curve from Fitzpatrick & Massa (2007) assuming $R_V = 3.1$. Then the light ratios in the Johnson *BVJHK* bands were derived using the WD models following G17, and employed to calculate the individual magnitudes and colors. Both the extinction correction and extrapolation of light ratios into the infrared add to uncertainty on derived intrinsic magnitudes. The extinction correction error is given in Table 4 but for the extrapolation uncertainty we did not add additional error. While for systems with similar temperature of components extrapolation leads to negligible additional error in some systems with the large temperature ratio of components this uncertainty may be significant. However when calculating a parallax (or a distance) to a particular eclipsing binary as an average from two components this uncertainty largely cancels out.

3.6. Photometric Parallaxes

The eclipsing binary method gives the photometric distance as well as the photometric parallax to a particular target, because both quantities are *inferred* from observables. Because of this we decided to work in a regime of parallaxes instead of distances to avoid an additional bias, which may arise in the conversion of parallaxes into distances. However, we underline here that working with a regime of parallaxes does not solve the whole problem because, for fractional parallax uncertainties larger then 15%–20%, the trigonometric parallax becomes a poor prior on the distance.

3.6.1. Parallaxes from the Bolometric Flux Scaling

In order to directly compare our results with those of Stassun & Torres (2018) we employed the bolometric flux scaling method utilizing the *V*-band bolometric corrections BC to derive photometric parallaxes. The photometric parallax ϖ to the ith component of the system was calculated using equation:

$$\varpi_i(\mathrm{mas}) = 2.956 \cdot 10^{10} R_i^{-1} T_i^{-2} \, 10^{-0.2(\mathrm{BC}_i + V_i)} \qquad (4)$$

where index $i = \{1, 2\}$, R is the radius of a component expressed in solar radii, T is its effective temperature, BC is a bolometric correction interpolated from the Flower (1996) tables for a given temperature and V is the intrinsic magnitude of a component. The parallax to a particular system was calculated as the unweighted average parallax of the two components.

3.6.2. Parallaxes from the SBC Relations

The eclipsing binary method of distance determination is very flexible and has many different approaches. We decided to use as our main approach the method based on the empirical surface brightness–color relations. In order to derive the photometric parallax to an eclipsing binary we need to calculate the individual angular diameters of the components. An angular diameter is calculated with the formula:

$$\phi(\mathrm{mas}) = 10^{0.2 \cdot (S - m_0)} \qquad (5)$$

where S is the surface brightness in a given band and m_0 is the dereddened magnitude of a star in that band. In most cases S is calibrated as a function of an intrinsic color of a star, usually in the form of a polynomial. The photometric parallax ϖ_{Phot} follows from the equation:

$$\varpi_{\mathrm{Phot}}(\mathrm{mas}) = 107.52 \cdot \phi(\mathrm{mas}) / R(\mathcal{R}_\odot), \qquad (6)$$

where R is the radius of the star and the conversion factor is equal to $1\,\mathrm{au}/2\,\mathcal{R}_\odot$ assuming the solar nominal radius $\mathcal{R}_\odot =$ 695,700 km (Habbereiter et al. 2008; Mamajek et al. 2015) and a length of the astronomical unit 1 au = 149,597,871 km (Pitjeva & Standish 2009).

We determined parallaxes using several SBC relations from the literature calibrated on infrared colors (Kervella et al. 2004; Di Benedetto 2005; Boyajian et al. 2014; Challouf et al. 2014). The most useful calibrations of S are based on $(B-K)$ and $(V-K)$ colors, because the reddening vector is almost parallel to the SBC relations for intermediate- and late-type stars. Moreover, these

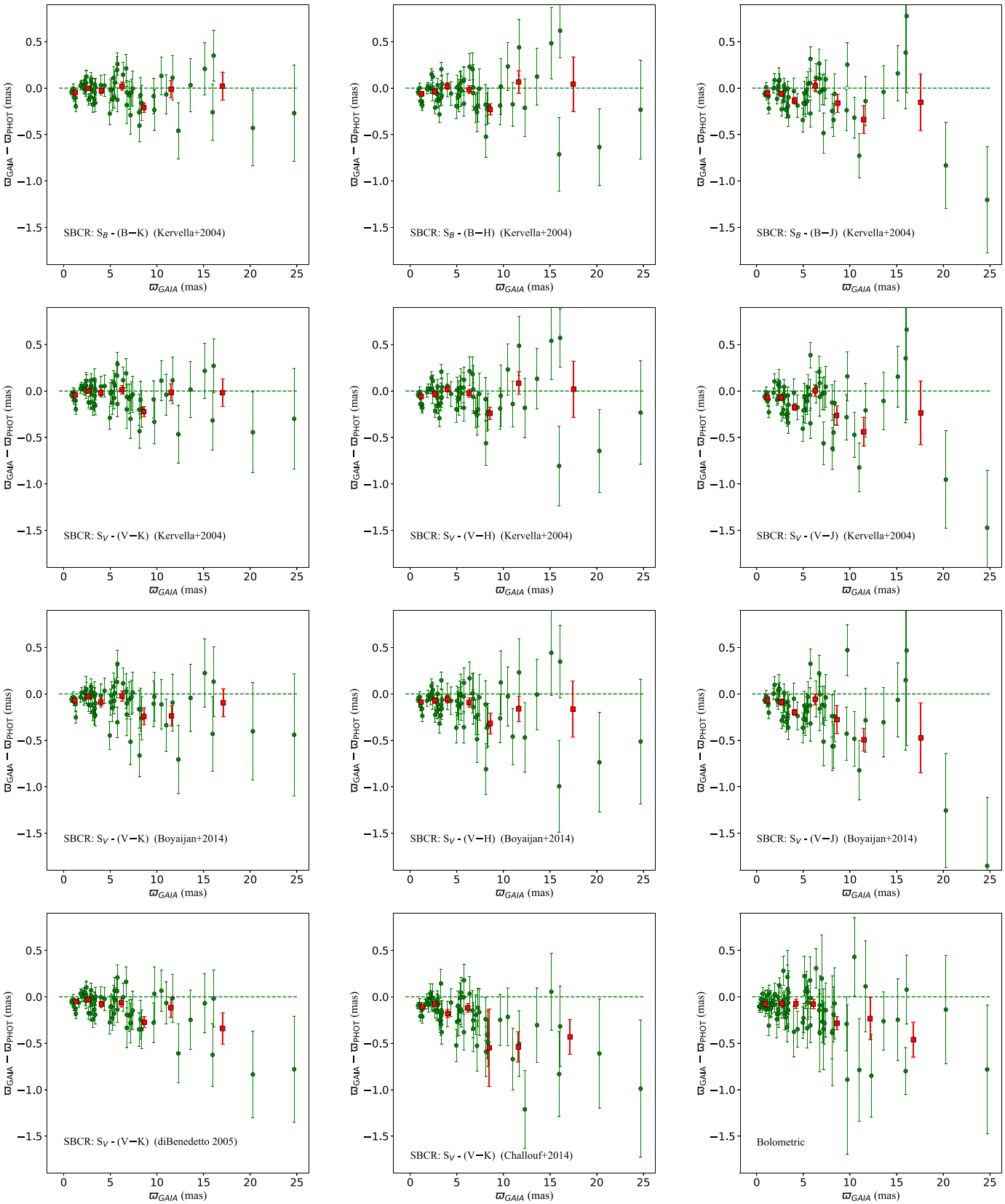

Figure 3. Individual parallax differences $d\varpi = \varpi_{Gaia} - \varpi_{\rm Phot}$ of eclipsing binaries as a function of the *Gaia* parallaxes for all SBC relations used (green circles). The red squares are binned weighted means. The direct comparison of ϖ_{Gaia} and $\varpi_{\rm Phot}$ for a few SBC relations is given in Figure 5.

relations have very low intrinsic dispersion (e.g., Kervella et al. 2004; Graczyk et al. 2017). However, we also used calibrations based on other infrared colors to have a more detailed view of possible systematics. The parallax to a given eclipsing binary was calculated as the unweighted average of the individual parallaxes of its components.

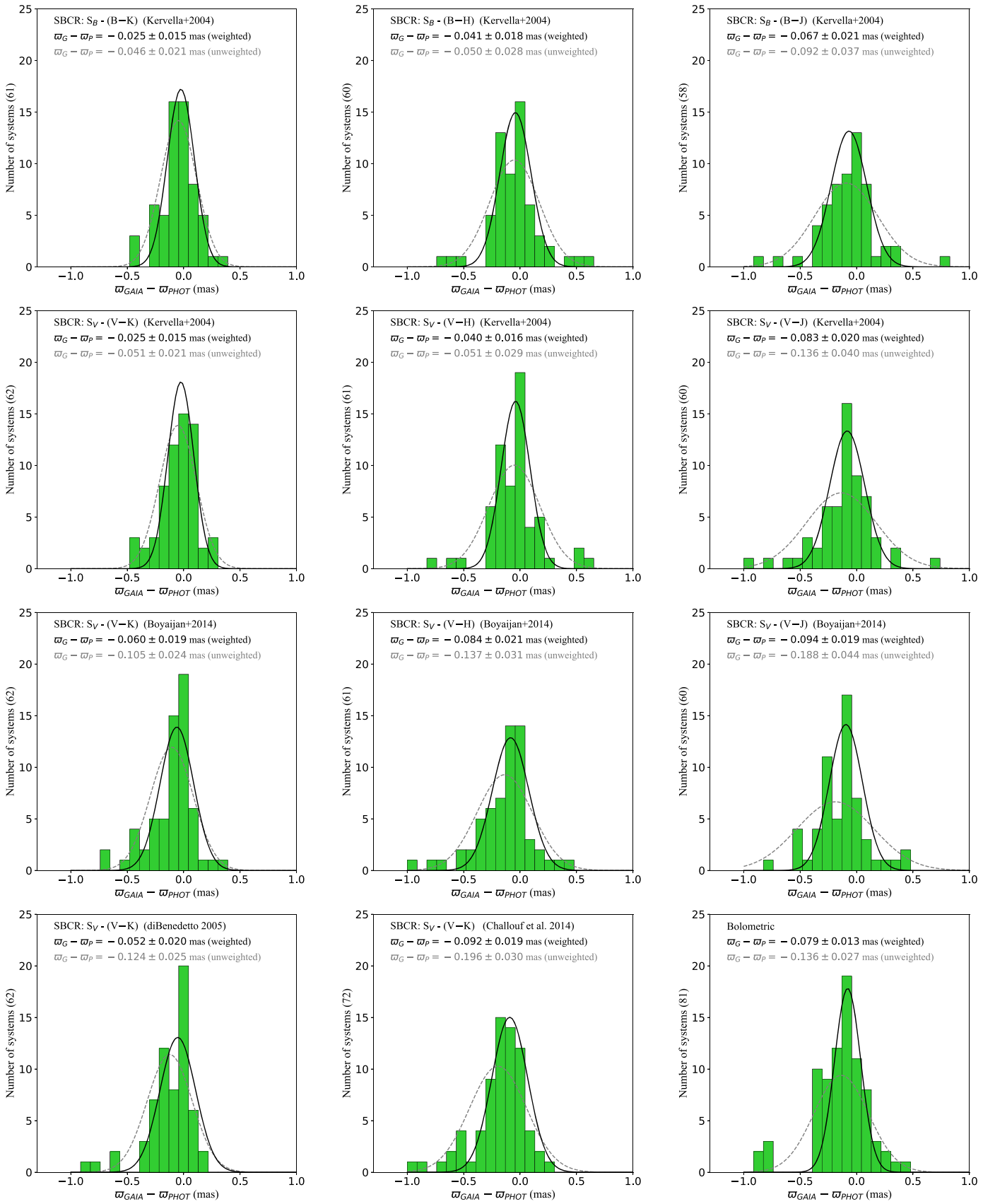

Figure 4. Histograms of the parallax differences $d\varpi = \varpi_{Gaia} - \varpi_{\rm Phot}$ for all SBC relations used. The Gaussian distributions correspond to weighted (continuous line) and unweighted (broken line) mean values. They are given just for a reference.

Table 5
The Zero-point Shifts $\varpi_{Gaia} - \varpi_{\rm Phot}$ Determined with Eclipsing Binaries for the Different SBCRs

SBC Relation	Band	Color	Range of Color	$\log g$ (dex)	Number of Systems	$(\varpi_{Gaia} - \varpi_{\rm Phot})$ (mas)	
						Unweighted	Weighted
Kervella et al. (2004)	B	$B-K$	−0.25 to 2.36	>3.5	61	-0.046 ± 0.021	-0.025 ± 0.015
Kervella et al. (2004)	B	$B-H$	−0.20 to 2.28	>3.5	60	-0.050 ± 0.028	-0.041 ± 0.018
Kervella et al. (2004)	B	$B-J$	−0.17 to 2.08	>3.5	58	-0.092 ± 0.037	-0.067 ± 0.021
Kervella et al. (2004)	V	$V-K$	−0.20 to 1.75	>3.5	62	-0.051 ± 0.021	-0.025 ± 0.015
Kervella et al. (2004)	V	$V-H$	−0.15 to 1.66	>3.5	61	-0.051 ± 0.029	-0.040 ± 0.016
Kervella et al. (2004)	V	$V-J$	−0.12 to 1.47	>3.5	60	-0.136 ± 0.040	-0.083 ± 0.020
Di Benedetto (2005)	V	$V-K$	−0.10 to 4.93	>2.0	62	-0.124 ± 0.025	-0.052 ± 0.020
Boyajian et al. (2014)	V	$V-K$	−0.15 to 1.75	>3.5	62	-0.105 ± 0.024	-0.060 ± 0.019
Boyajian et al. (2014)	V	$V-H$	−0.13 to 1.66	>3.5	61	-0.137 ± 0.031	-0.084 ± 0.021
Boyajian et al. (2014)	V	$V-J$	−0.12 to 1.47	>3.5	60	-0.188 ± 0.044	-0.094 ± 0.019
Challouf et al. (2014)	V	$V-K$	−0.60 to 4.93	>2.0	72	-0.196 ± 0.030	-0.092 ± 0.019
Bolometric	...	...	...	...	81	-0.103 ± 0.026	-0.067 ± 0.012

Note. The blue edge of the color range is constrained by the color range validity of the SBC relation (with the exception of the relation by Challouf et al. 2014) and the red range is contrained by most red systems in the sample.

3.7. Calculation of the Shift with Respect to Gaia Parallaxes

We calculated individual parallax differences $d\varpi_i = (\varpi_{Gaia} - \varpi_{\rm Phot})_i$ for every ith eclipsing binary and for each SBC relation used. For a given SBC relation we then determined the zero-point shift between the photometric and *Gaia* parallaxes as unweighted and weighted means of the differences. The individual differences for all used SBC relations are presented in Figure 3. The errors of the differences were calculated taking into account systematic uncertainties of the SBC relations: 2% for calibrations by Kervella et al. (2004) and Di Benedetto (2005), 3% for calibrations by Boyajian et al. (2014), and 3.5% for calibration by Challouf et al. (2014)—their Equation (13). Weighted means are dominated by more distant systems for which the error on $d\varpi$ is much smaller than for nearby eclipsing binaries. This is a bit counterintuitive and it needs an explanation. Error on $d\varpi$ comes from two uncertainties: that of the *Gaia* parallax and that of the eclipsing binary photometric parallax. While the former for stars with $G < 14$ mag (all our sample) is almost independent of the distance and equal to 0.04 mas on average (Lindegren et al. 2018), the latter decreases with the distance because it is, in the majority of cases, dominated by a systematic uncertainty of the SBCR. Thus for a systematic error of 2% on the photometric parallax the uncertainty is about 0.2 mas for a system lying 100 pc from the Sun and about 0.02 mas for a system lying 1 kpc away. In Figure 4 we present histograms of the differences for all the SBCR used, and also for parallaxes derived with the bolometric flux scaling method. The Gaussians correspond to a standard uncertainty distribution on weighted (continuous line) and unweighted means (dashed line).

4. Results

Table 5 presents a summary of the zero-point $\varpi_{Gaia} - \varpi_{\rm Phot}$ shifts for the different SBC relations, and in Figure 5 we show exemplary relations between trigonometric *Gaia* DR2 and photometric, eclipsing binary parallaxes. The photometric parallaxes derived from bolometric fluxes correspond well with *Gaia* DR2 parallaxes, although the offset between both is clear. The amount of the offset of -0.067 ± 0.012 mas is marginally consistent with the zero-point shift reported by Stassun & Torres (2018). Our sample agrees in about 80% with a sample used by Stassun & Torres (2018), we also adopted the same solar constants; however, we used a different method to derive $L_{\rm bol}$, which may account for the difference with their result. We point out that the accuracy of the derived offset is limited by the accuracy of the zero-points of the different methods used to determine the effective temperatures and the choice of solar constants. However, the problem of homogenization of the temperature determination for all the sample and the proper calibration of the temperature zero-point scale is beyond the scope of this paper. We therefore prefer to establish the *Gaia* zero-point shift solely based on the empirical SBC relations, which allows for a homogenous treatment of the sample (and its subsamples).

As pointed out already by Stassun & Torres (2018) there is almost perfect agreement between the photometric and *Gaia* DR2 parallaxes. However, some of the SBC relations result in a larger offset and larger differences (e.g., Challouf et al. 2014)—see Figures 3 and 4. The possible reasons for this are discussed in the next section.

The SBC relations, which result in the smallest differences and best agreement with *Gaia* DR2 parallaxes are those based on $(B-K)$ and $(V-K)$ colors and calibrated by Kervella et al. (2004). They are also the relations that result in the smallest internal dispersions of the differences. Calibrations based on these two colors are the least reddening dependent because the reddening line on the surface brightness S–color diagram is almost parallel to the relations themselves. Moreover, the calibrations by Kervella et al. (2004) were done for main-sequence dwarfs and subgiants, which constitute the overwhelming majority of the eclipsing binary component stars in our sample. The resulting zero-point shift based on the $(B-K)$ and $(V-K)$ relations is -0.025 ± 0.011 mas. Relations by Kervella et al. (2004) calibrated on the other optical-infrared colors are more reddening dependent and also show significantly larger scatter of the differences.

Another SBC relation that we used extensively for the determination of the distances to the Magellanic Clouds

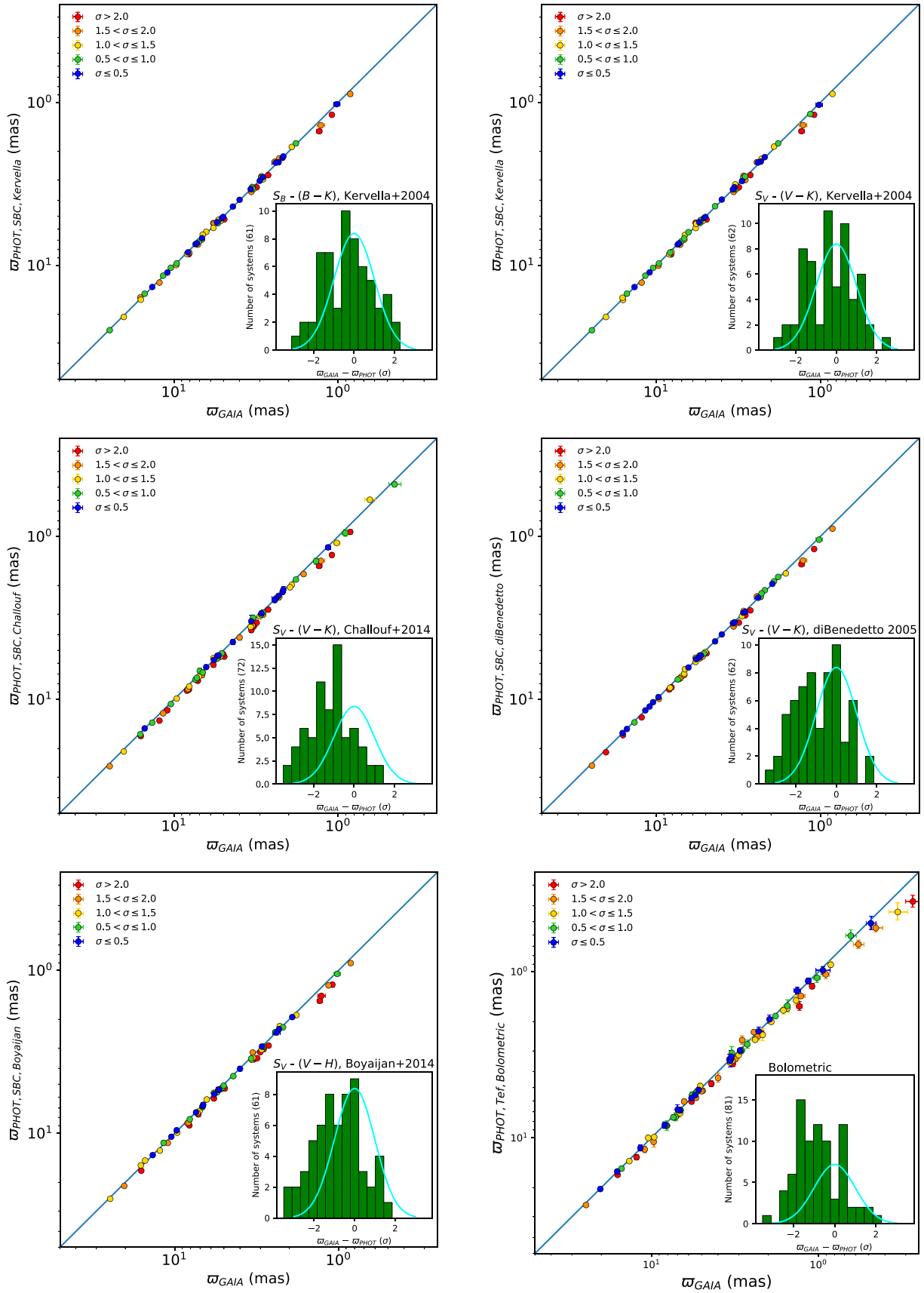

Figure 5. Direct comparison of the *Gaia* and the photometric parallaxes for a few SBC relations. The errorbars in most cases are smaller than the size of the symbols. Insets show histograms like in Figure 4 but expressed in terms of uncertainty of $d\varpi$. The Gaussians show the expected distribution if no offset is present.

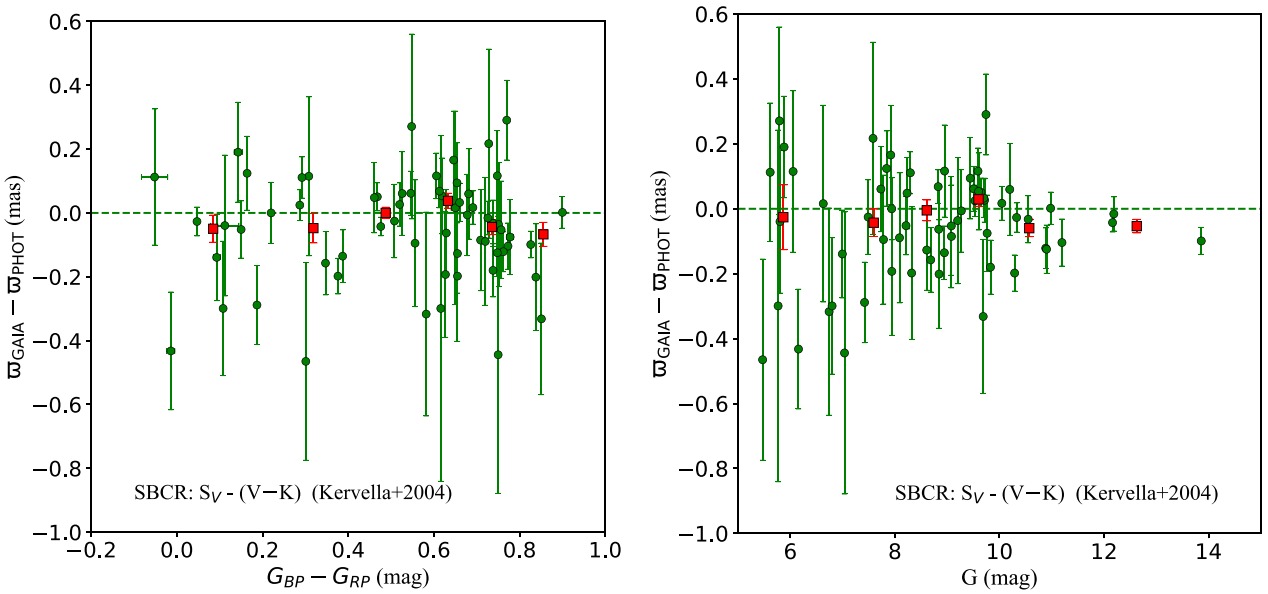

Figure 6. Color and magnitude dependency of the parallax differences for the SBC relation by Kervella et al. (2004). The meanings of the symbols are the same as in Figure 3.

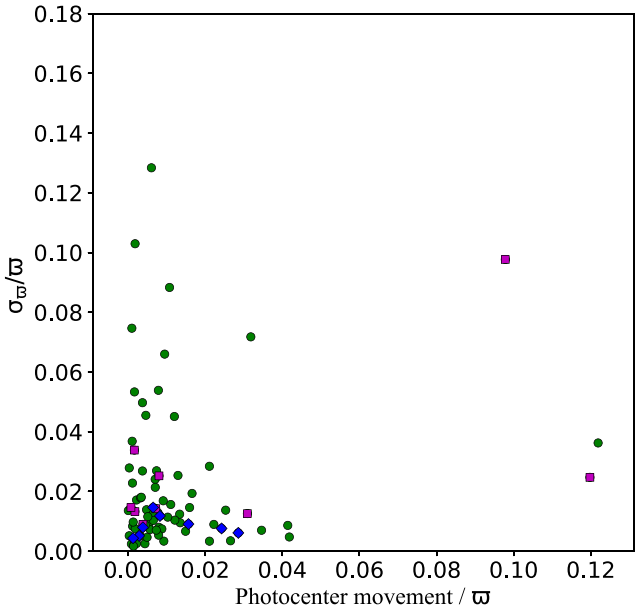

Figure 7. Photocenter movement of eclipsing binaries in our sample expressed as a fraction of *Gaia* DR2 parallax vs. the fractional uncertainty of the *Gaia* parallax. The meanings of the symbols are the same as in Figure 1.

(Pietrzyński et al. 2013; Graczyk et al. 2014) was calibrated by Di Benedetto (2005). This relation is calibrated on a mixture of giant and dwarf stars. The resulting zero-point shift is $d\varpi = -0.052 \pm 0.020$ mas and is within 1.3σ consistent with the $d\varpi$ derived from the Kervella et al. SBC relations. Combining these two determinations we obtain a value of $d\varpi = -0.031 \pm 0.011$.

5. Discussion

Using the most reliable SBC relations available in the literature, we derived a zero-point shift for *Gaia* DR2 parallaxes of $d\varpi = -0.031 \pm 0.011$ mas. However, there are significant differences of the zero-point shifts resulting from applying (1) different SBC calibrations, and (2) different colors.

The reasons for the existence of the SBC calibration dependent zero-point shifts are somewhat unclear. A choice of different interferometric stellar angular diameter sets will result in different calibrations. Most notably a calibration derived from a mixture of all kinds of stars (e.g., Challouf et al. 2014) may lead to a systematic difference with a calibration based on a mixture of dwarf and subgiant stars only (e.g., Kervella et al. 2004). However, more worrisome is a systematic difference of the zero-point shifts derived from the same colors but from two different calibrations (Kervella et al. 2004; Boyajian et al. 2014) that are based on angular diameters of dwarf and subgiants stars and calibrated on the Johnson system. We searched relevant papers to find the differences. Kervella et al. (2004) use a small but well characterized sample of stars, while Boyajian et al. (2014) used a much larger sample but containing multiple and variable stars, and also utilizing saturated 2MASS photometry for some bright stars. Because of this we tend to prefer the former calibrations over the latter. The systematic differences between the calibrations (see Table 5) vary from −0.011 to −0.044 mas with a weighted average of −0.031 mas.

Regarding (2) there is a clear trend that relations calibrated on shorter-wavelength colors (and therefore being more reddening dependent) give systematically larger zero-point shifts and larger scatter of the differences, with the largest shifts coming from SBC relation calibrations based on the $(V-J)$ color. We tried to remove the shifts by a rescaling of all individual reddening estimates according to $E(B-V)_{\rm new} = C \cdot E(B-V)$, where $C > 1$ is a scaling factor. Unless C is larger then about 4 there is no possibility to obtain an agreement between zero-point shifts derived from different colors. But such a large value of the scaling factor would lead to an unrealistically large extinction for most of the targets in our sample, and would be strongly at odds with independent reddening determinations by Stassun & Torres (2016).

Another, but less likely, possibility is that the transformation equations from Section 2.1.2 contain some systematic error leading to color dependent zero-point shifts. And at last the SBC relations calibrated on colors containing J and H may be problematic by themselves because of a proper calibration of the ground-based photometry in these filters is difficult (strong and variable atmospheric extinction) and because of stronger sensibility to the interstellar reddening.

We investigated how the global shift depends on a distance. We binned up individual $d\varpi_i$ in several bins—see Figure 3; however, no clear systematic trend can be noticed. We also investigated a possible *Gaia* color $G_{BP} - G_{RP}$ and G magnitude dependency. We plotted $d\varpi$ differences for one specific SBC relation—Figure 6. As previously we do not detect any systematic trend. We also investigated the correlation of $d\varpi$ with sky position. We calculated separately shifts for equatorial and ecliptic hemispheres. The differences between hemispheres are in both cases within 1σ uncertainty and thus not statistically significant.

The comparison with previous determinations of $d\varpi$ shows excellent agreement with the *Gaia* Team results (Arenou et al. 2018; Lindegren et al. 2018). In fact we confirm here the zero-point shift of $d\varpi = -0.029$ mas reported by the *Gaia* Team. However, comparisons with other independent determinations show some discrepancies. Although the $d\varpi$ value reported by Riess et al. (2018) agrees with our value at the 1σ level, the zero-point shifts reported by Stassun & Torres (2018) and Zinn et al. (2018) are somewhat discrepant. The problem with the shift reported by Zinn et al. (2018) is its unrealistically small systematic uncertainty, which ignores systematics of asteroseismic relations themselves and the zero-point uncertainty of the temperature scale used by the authors. Because of this a comparison of the shift by Zinn et al. (2018) with other reported shifts is vague.

Of special interest is the knowledge of how binarity will impact *Gaia* parallaxes, and the determination of the global zero-point shift. In order to quantify this, we calculated the photocenter movement for our ∼80 eclipsing binaries and compared them with the uncertainties on *Gaia* DR2 parallaxes —see Figure 7. For the overwhelming majority of the systems the photocenter movement is only a very small fraction of the parallax itself. Only in two systems could *Gaia* DR2 probably recognize the photocenter movement (EPIC 211409263 and V380 Cyg). Thus we can consider the *Gaia* DR2 parallaxes of the eclipsing binaries in our sample as practically unaffected by binarity.

We dedicate this paper to our colleague Zbigniew ("Zibi") Kołaczkowski who passed away much too early.

We thank the anonymous referee for valuable comments and remarks on the manuscript. The research leading to these results has received funding from the European Research Council (ERC) under the European Union's Horizon 2020 research and innovation program (grant agreement No. 695099).

We are grateful for financial support from Polish National Science Center grant MAESTRO 2012/06/A/ST9/00269. Support from the BASAL Centro de Astrofísica y Tecnologías Afines (CATA) grant AFB-170002, the Millenium Institute of Astrophysics (MAS) of the Iniciativa Cientifica Milenio del Ministerio de Economia, Fomento y Turismo de Chile, project IC120009 and the IdP II 2015 0002 64 grant of the Polish Ministry of Science and Higher Education is also acknowledged. We are also thankful to the staff in La Silla Observatory (ESO) and Las Campanas Observatory (Carnegie) for their excellent support.

This work has made use of data from the European Space Agency (ESA) mission *Gaia* (https://www.cosmos.esa.int/gaia), processed by the *Gaia* Data Processing and Analysis Consortium (DPAC, https://www.cosmos.esa.int/web/gaia/dpac/consortium). Funding for the DPAC has been provided by national institutions, in particular, the institutions participating in the *Gaia* Multilateral Agreement.

This research has made extensive use of the excellent astronomical SIMBAD database and of the VizieR catalog access tool, operated at CDS, Strasbourg, France, and made also use of NASA's Astrophysics Data System Bibliographic Services (ADS).

This publication makes use of data products from the Two Micron All Sky Survey, which is a joint project of the University of Massachusetts and the Infrared Processing and Analysis Center/California Institute of Technology, funded by the National Aeronautics and Space Administration and the National Science Foundation.

ORCID iDs

Dariusz Graczyk https://orcid.org/0000-0002-7355-9775
Wolfgang Gieren https://orcid.org/0000-0003-1405-9954
Jesper Storm https://orcid.org/0000-0002-8627-6096
Nicolas Nardetto https://orcid.org/0000-0002-7399-0231
Alexandre Gallenne https://orcid.org/0000-0001-7853-4094
Pierre F. L. Maxted https://orcid.org/0000-0003-3794-1317
Pierre Kervella https://orcid.org/0000-0003-0626-1749
Bogumił Pilecki https://orcid.org/0000-0003-3861-8124
Paulina Karczmarek https://orcid.org/0000-0002-0136-0046
Mónica Taormina https://orcid.org/0000-0002-1560-8620
Piotr Wielgórski https://orcid.org/0000-0002-1662-5756
Radosław Smolec https://orcid.org/0000-0001-7217-4884

References

Albrecht, S., Reffert, S., Snellen, I., Quirrenbach, A., & Mitchell, D. S. 2007, A&A, 474, 565
Albrecht, S., Reffert, S., Snellen, I. A. G., & Winn, J. N. 2009, Natur, 461, 373
Albrecht, S., Sewiatan, J., Torres, G., Fabrycky, D. C., & Winn, J. N. 2013, ApJ, 767, 32
Albrecht, S., Winn, J. N., Torres, G., et al. 2014, ApJ, 785, 83
Andersen, J. 1975, A&A, 44, 355
Andersen, J., & Clausen, J. V. 1989, A&A, 213, 183
Andersen, J., Clausen, J. V., & Giménez, A. 1993, A&A, 277, 439
Andersen, J., Clausen, J. V., & Magain, P. 1989, A&A, 211, 346
Andersen, J., Clausen, J. V., & Nordstrom, B. 1984, A&A, 137, 281
Andersen, J., Clausen, J. V., & Nordström, B. 1987a, A&A, 175, 60
Andersen, J., Clausen, J. V., Nordstrom, B., & Popper, D. M. 1985, A&A, 151, 329
Andersen, J., Clausen, J. V., Nordström, B., & Reipurth, B. 1983, A&A, 121, 271
Andersen, J., Clausen, J. V., Nordström, B., Tomkin, J., & Mayor, M. 1991, A&A, 246, 99
Andersen, J., García, J. M., Giménez, A., & Nordström, B. 1987b, A&A, 174, 107
Andersen, J., Gjerløff, H., & Imbert, M. 1975, A&A, 44, 349
Andersen, J., & Vaz, L. P. R. 1984, A&A, 130, 102
Arenou, F., Luri, X., Babusiaux, C., et al. 2018, A&A, 616, 17
Bailer-Jones, C. A. L. 2015, PASP, 127, 994
Bailer-Jones, C. A. L., Rybizky, J., Fouesneau, M., Mantelet, G., & Andrae, R. 2018, AJ, 156, 58
Bakiş, V., Bakiş, H., Bilir, S., & Eker, Z. 2016, PASA, 33, 46

Bakiş, V., Bakiş, H., Demircan, O., & Eker, Z. 2008, MNRAS, 384, 1657
Barembaum, M. J., & Etzel, P. B. 1995, AJ, 109, 2680
Bessell, M. 2000, PASP, 112, 961
Bessell, M. S., & Brett, J. M. 1988, PASP, 100, 1134
Bilir, S., Ak, T., Soydugan, E., et al. 2008, AN, 329, 835
Boyajian, T. S., van Belle, G., & von Braun, K. 2014, AJ, 147, 47
Budding, E., Butland, R., & Blackford, M. 2015, MNRAS, 448, 3784
Capitanio, L., Lallement, R., Vergely, J. L., Elyajouri, M., & Monreal-Ibero, A. 2017, A&A, 606, 65
Carpenter, J. M. 2001, AJ, 121, 2851
Casagrande, L., Portinari, L., Glass, I. S., et al. 2014, MNRAS, 439, 2060
Challouf, M., Nardetto, N., Mourard, D., et al. 2014, A&A, 570, 104
Clausen, J. V. 1991, A&A, 246, 397
Clausen, J. V., Bruntt, H., Olsen., E. H., Helt, B. E., & Claret, A. 2010, A&A, 511, 22
Clausen, J. V., Frandsen, S., Bruntt, H., et al. 2010, A&A, 516, 42
Clausen, J. V., Giménez, A., & Scarfe, C. 1986, A&A, 167, 287
Clausen, J. V., Helt, B. E., Gimenez, A., et al. 2007, A&A, 461, 1065
Clausen, J. V., Helt, B. E., & Olsen, E. H. 2001, A&A, 374, 980
Clausen, J. V., Torres, G., Bruntt, H., et al. 2008, A&A, 487, 1095
David, T. J., Conroy, K. E., Hillenbrand, L. A., et al. 2016, AJ, 151, 112
Demircan, O., Kaya, Y., & Tufekcioglu, Z. 1994, Ap&SS, 222, 213
Di Benedetto, G. P. 2005, MNRAS, 357, 174
Eker, Z., Bilir, S., Soydugan, F., et al. 2014, PASA, 31, 24
Fekel, F. C., Williamson, M. H., & Henry, G. W. 2011, AJ, 141, 145
Fitzpatrick, E. L., & Massa, D. 2007, ApJ, 663, 320
Flower, P. J. 1996, ApJ, 469, 355
Gaia Collaboration, Brown, A. G. A., Vallenari, A., Prusti, T., et al. 2018, A&A, 616, 1
Gaia Collaboration, Prusti, T., de Bruijne, J. H. J., Brown, A. G. A., et al. 2016, A&A, 595, 1
Gallenne, A., Pietrzyński, G., Graczyk, D., et al. 2016, A&A, 586, 35
Giuricin, G., Mardirossian, F., Mezzetti, M., & Predolin, F. 1980, A&A, 85, 259
Graczyk, D., Konorski, P., Pietrzyński, G., et al. 2017, ApJ, 837, 7
Graczyk, D., Pietrzyński, G., Thompson, I. B., et al. 2014, ApJ, 780, 59
Graczyk, D., Smolec, R., Pavlovski, K., et al. 2016, A&A, 594, 92
Griffin, R. F. 2013, Obs, 133, 156
Groenewegen, M. A. T. 2018, arXiv:1808.05796
Groenewegen, M. A. T., Decin, L., Salaris, M., & De Cat, P. 2007, A&A, 463, 579
Gronbech, B., Gyldenkerne, K., & Jorgensen, H. E. 1977, A&A, 55, 401
Habbereiter, M., Schmutz, W., & Kosovichev, A. G. 2008, ApJ, 675, 53
Harmanec, P., Holmgren, D. E., Wolf, M., et al. 2014, A&A, 563, 120
Hełminiak, K. G., Konacki, M., Ratajczak, M., & Muterspaugh, M. W. 2009, MNRAS, 400, 969
Hełminiak, K. G., Ukita, N., Kambe, E., & Konacki, M. 2015, ApJ, 813, 25
Henry, G. W., Fekel, F. C., Sowell, J. R., & Gearhart, J. S. 2006, AJ, 132, 2489
Høg, E., Fabricius, C., Makarov, V. V., et al. 2000, A&A, 357, 367
Çakirli, Ö, Ibanoğlu, C., Bilir, S., & Sipahi, E. 2009, MNRAS, 395, 1649
Imbert, M. 1985, A&AS, 59, 357
Imbert, M. 1986, A&AS, 65, 97
Imbert, M. 1987, A&AS, 69, 397
Imbert, M. 2002, A&A, 387, 850
Kervella, P., Arenou, F., Mignard, F., & Thevenin, F. 2019, A&A, in press (arXiv:1811.08902)
Kervella, P., Thévenin, F., Di Folco, E., & Ségransan, D. 2004, A&A, 426, 297
Khaliullin, K. F., Khaliullina, A. I., & Krylov, A. V. 2001, ARep, 45, 888
Kirkby-Knet, J. A., Maxted, P. F. L., Serenelli, A. M., et al. 2018, A&A, 615, 135
Kurucz, R. 1993, ATLAS9 Stellar Atmosphere Programs and 2 km s^{-1} Grid, Kurucz CD-ROM No. 13 (Cambridge, MA: SAO)
Lacy, C. H. 1987, AJ, 94, 1670
Lacy, C. H., & Frueh, M. L. 1985, ApJ, 295, 569
Lacy, C. H., & Frueh, M. L. 1987, ApJ, 94, 712
Lacy, C. H., Gülmen, O., Güdür, N., & Sezer, C. 1989, AJ, 97, 822
Lacy, C. H. S. 1997, AJ, 113, 1406
Lacy, C. H. S. 2002, AJ, 124, 1162
Lacy, C. H. S., Claret, A., & Sabby, J. A. 2004a, AJ, 128, 1340
Lacy, C. H. S., Claret, A., & Sabby, J. A. 2004b, AJ, 128, 1840
Lacy, C. H. S., Claret, A., Sabby, J. A., Hood, B., & Secosan, F. 2004c, AJ, 128, 3005
Lacy, C. H. S., & Fekel, F. C. 2011, AJ, 142, 185
Lacy, C. H. S., & Fekel, F. C. 2014, AJ, 148, 71
Lacy, C. H. S., Fekel, F. C., & Claret, A. 2012, AJ, 144, 63
Lacy, C. H. S., Torres, G., Claret, A., et al. 2000, AJ, 119, 1389
Lacy, C. H. S., Torres, G., & Claret, A. 2008, AJ, 135, 1757
Lacy, C. H. S., Torres, G., Claret, A., & Menke, J. L. 2006, AJ, 131, 2664
Lacy, C. H. S., Torres, G., Fekel, F. C., & Muterspaugh, M. W. 2014, AJ, 147, 148
Lacy, C. H. S., Torres, G., Fekel, F. C., Sabby, J. A., & Claret, A. 2012, AJ, 143, 129
Lallement, R., Vergely, J.-L., Valette, B., et al. 2014, A&A, 561, 91
Latham, D. W., Nordstroem, B., Andersen, J., et al. 1996, A&A, 314, 864
Lester, K. V., & Gies, D. R. 2018, AJ, 156, 8
Lindegren, L., Hernández, J., Bombrun, A., et al. 2018, A&A, 616, 2
Mamajek, E. E., Prsa, A., Torres, G., et al. 2015, IAU 2015 Resolution B3, arXiv:1510.07674
Maxted, P. F. L., Hutcheon, R. J., Torres, G., et al. 2015, A&A, 578, 25
Mermilliod, J. C. 1997, yCat, 2168, 0
Munari, U., Dallaporta, S., Siviero, A., et al. 2004, A&A, 418, L31
Muraveva, T., Delgado, H. E., Clementini, G., Sarro, L. M., & Garofalo, A. 2018, arXiv:1805.08742
North, P., Studer, M., & Kunzli, M. 1997, A&A, 324, 137
Ochsenbein, F., Bauer, P., & Marcout, J. 2000, A&AS, 143, 23
Pavlovski, K., Southworth, J., Kolbas, V., & Smalley, B. 2014, MNRAS, 438, 590
Pavlovski, K., Tamajo, E., Koubský, P., et al. 2009, MNRAS, 400, 791
Pietrzyński, G., Graczyk, D., Gieren, W., et al. 2013, Natur, 495, 76
Pitjeva, E. V., & Standish, E. M. 2009, CeMDA, 103, 356
Popper, D. M. 1971, ApJ, 169, 549
Popper, D. M. 1982, ApJ, 254, 203
Popper, D. M. 1983, AJ, 88, 1242
Popper, D. M. 1987, AJ, 93, 672
Popper, D. M. 1998, AJ, 115, 338
Popper, D. M., Andersen, J., Clausen, J. V., & Nordstrom, B. 1985, AJ, 90, 1324
Popper, D. M., Lacy, C. H., Frueh, M. L., & Turner, A. E. 1986, AJ, 91, 383
Pribulla, T., Merand, A., Kervella, P., et al. 2018, A&A, 616, 49
Ratajczak, M., Kwiatkowski, T., Schwarzenberg-Czerny, A., et al. 2010, MNRAS, 402, 2424
Rawls, M. L., Gaulme, P., McKeever, J., et al. 2016, ApJ, 818, 108
Ribas, I., Jordi, C., & Jordi, T. 1999, MNRAS, 309, 199
Riess, A. G., Casertano, S., Yuan, W., et al. 2018, ApJ, 861, 126
Sabby, J. A., Lacy, C. H. S., Ibanoglu, C., & Claret, A. 2011, AJ, 141, 195
Sandquist, E. L., Jessen-Hansen, J., Shetrone, M. D., et al. 2016, ApJ, 831, 11
Sandquist, E. L., Mathieu, R. D., Quinn, S. N., et al. 2018, AJ, 155, 152
Schlegel, D. J., Finkbeiner, D. P., & Davis, M. 1998, ApJ, 500, 525
Skrutskie, M. F., Cutri, R. M., Stiening, R., et al. 2006, AJ, 131, 1163
Southworth, J. 2013, A&A, 557, 119
Southworth, J. 2015, in ASP Conf. Ser. 496, Living Together: Planets, Host Stars and Binaries, ed. S. Rucinski, G. Torres, & M. Zejda (San Francisco, CA: ASP), 164
Southworth, J., & Clausen, J. V. 2007, A&A, 461, 1077
Southworth, J., Maxted, P. F. L., & Smalley, B. 2005, A&A, 429, 645
Southworth, J., Pavlovski, K., Tamajo, E., et al. 2011, MNRAS, 414, 3740
Southworth, J., Smalley, B., Maxted, P. F. L., Claret, A., & Etzel, P. B. 2005, MNRAS, 363, 529
Sowell, J. R., Henry, G. W., & Fekel, F. C. 2012, AJ, 143, 5
Stassun, K. G., & Torres, G. 2016, AJ, 152, 180
Stassun, K. G., & Torres, G. 2018, ApJ, 862, 61
Stickland, D. J., Lloyd, C., & Corcoran, M. F. 1994, Obs, 114, 284
Suchomska, K., Graczyk, D., Smolec, R., et al. 2015, MNRAS, 451, 651
Tkachenko, A., Degroote, P., Aerts, C., et al. 2014, MNRAS, 438, 3093
Tomasella, L., Munari, U., Cassisi, S., et al. 2008a, A&A, 483, 263
Tomasella, L., Munari, U., Siviero, A, et al. 2008b, A&A, 480, 465
Tomkin, J., & Fekel, F. C. 2006, AJ, 131, 2652
Torres, G., Andersen, J., & Giménez, A. 2010, A&ARv, 18, 67
Torres, G., Andersen, J., Nordström, B., & Latham, D. W. 2000, AJ, 119, 1942
Torres, G., & Lacy, C. H. S. 2009, AJ, 137, 507
Torres, G., Lacy, C. H. S., Claret, A., et al. 1999, AJ, 118, 1831
Torres, G., Lacy, C. H. S., & Claret, A. 2009, AJ, 138, 1622
Torres, G., Lacy, C. H. S., Pavlovski, K., et al. 2014, ApJ, 797, 31
Torres, G., Lacy, C. H. S., Pavlovski, K., Fekel, F. C., & Muterspaugh, M. W. 2015, AJ, 150, 154
Torres, G., McGruder, C. D., Siverd, R. J., et al. 2017, ApJ, 836, 177
van Hamme, W., & Wilson, R. E. 2007, ApJ, 661, 1129
Veramendi, M. E., & González, J. F. 2015, NewA, 34, 266
Vos, J., Clausen, J. V., Jørgensen, U. G., et al. 2012, A&A, 540, 64
Walker, R. L., & Chambliss, C. R. 1983, AJ, 88, 535
Williamon, R. M., Sowell, J. R., & van Hamme, W. 2004, AJ, 128, 1319
Wilson, R. E. 1979, ApJ, 234, 1054
Wilson, R. E. 1990, ApJ, 356, 613
Wilson, R. E., & Devinney, E. J. 1971, ApJ, 166, 605
Worthey, G., & Lee, H. 2011, ApJS, 193, 1
Yakut, K., Aerts, C., & Morel, T. 2007, A&A, 467, 647
Zinn, J. C., Pinsonneault, M. H., Huber, D., & Stello, D. 2018, arXiv:1805.02650